Korean J. Chem. Eng., **26**(2), 359-363 (2009)

CFD modeling of shell-and-tube heat exchanger header for uniform distribution among tubes

Myoung Il Kim*, Yoong Lee*, Byung Woo Kim*, Dong Hyun Lee*,†, and Won Seob Song**

*Department of Chemical Engineering, Sungkyunkwan University, Suwon 440-746, Korea
**Production & Technology Center, Samsung Fine Chemicals Co. Ltd., Ulsan 680-090, Korea
(*Received 6 July 2008 • accepted 25 August 2008*)

Abstract−Several different designs for a header type were numerically studied to achieve uniform distribution of gas phase flow in the header of a shell-and-tube heat exchanger. The different geometries included the position and shape of the inlet nozzle, number of outlet tubes, and length. In numerical calculations, the k-epsilon realizable turbulent model was employed. Standard deviation was used to evaluate the uniformity of the velocity distribution among the whole outlets of the header. As a result, flow patterns in the header could be visualized by using post-processing of numerical results. The uniformity of flow distribution increased with header length, whereas it decreased with gas flow rate. Furthermore, the optimum position and shape of the inlet nozzle could be proposed for a uniform distribution of a 1.3 m-length header, the very same used for the heat exchange of the commercially viable allyl chloride process.

Key words: CFD, Shell-and-tube Heat Exchanger, Header, Distribution

INTRODUCTION

At least 60% of heat exchanger types are the shell-and-tube type exchanger, indicating its prevalence in the process industry [1], with applications in oil coolers and power condensers, as well as preheaters in power plants and steam generators in nuclear power plants, process applications, and the chemical industry [2]. One of the most common assumptions in basic heat exchanger design theory is that fluid can be distributed uniformly at the inlet of the exchanger on each fluid side and throughout the core. In general, flow rates through the channels are not uniform and, in extreme cases, there is almost no flow through some, exhibiting poor heat exchange performance [3].

Maldistribution of flow, which can take place in the header, can cause a change of local heat flow and directly affect the performance of total heat transfer [4]. Much research has been focused upon understanding the characteristics of velocity distribution and to improve its uniformity.

In Eq. (1), Fraas et al. [5] described the extent of maldistribution using the velocity ratio between maximum and minimum value in the tube:

$$\eta = \sqrt{\frac{0.5\rho V_0^2 + \Delta p_{av}}{\Delta p_{av}}} \quad (1)$$

where, Δp_{av} is the average pressure drop in the heat exchanger and $0.5\rho V_0^2$ is the dynamic pressure of inlet nozzle. Eq. (1) indicates that the velocity distribution becomes uniform as the average pressure drop increases.

Lalot et al. [6] performed experimental and computational works concerning velocity distribution in an electrical heater. They reported that the computed velocity ratio (maximum velocity/minimum velocity) deviated less than 5% from the experimental.

Vist et al. [7] classified the parameters of fluidization distribution into operating parameters, such as mass flux and heat quantity at each pipe, and geometric parameters, such as tube diameter/direction and inlet length.

In this present study, CFD (Computational Fluid Dynamics) modeling for flow patterns in different header types was used to investigate the characteristics of their velocity distribution in a shell-and-tube heat exchanger, and the effectiveness of the simulated results in an actual heat exchanger was also evaluated.

NUMERICAL ANALYSIS

The commercial package, FLUENT 6, was used as a CFD solver [8]. Three-dimensional plane symmetric geometry was considered with the tetrahedral-meshing scheme. A schematic diagram of shell-and-tube heat exchanger header is shown in Fig. 1. This header (1.05 m-ID) has one inlet nozzle (0.25 m-ID), 80 tube side outlets (0.08 m-ID) and a 2 : 1 ellipsoid head. From this basic shape, the header length

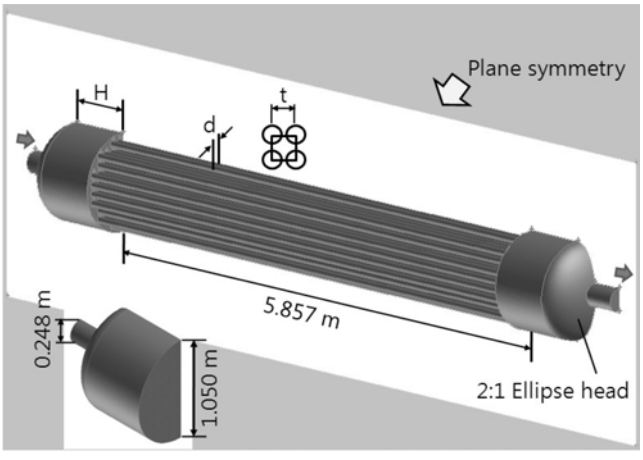

Fig. 1. Schematic of the shell-and-tube type heat exchanger.

†To whom correspondence should be addressed.
E-mail: dhlee@skku.edu

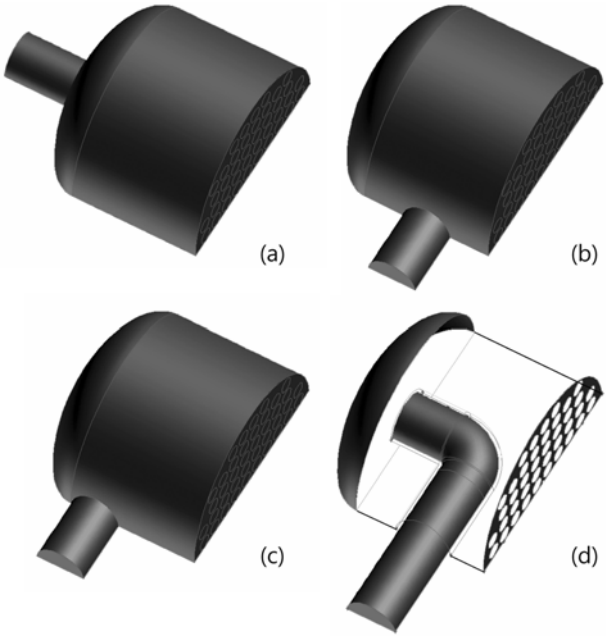

Fig. 2. Different header configurations of the shell-and-tube type heat exchanger. (a) A-type header, (b) B-type header, (c) C-type header, and (d) D-type header.

Table 1. CFD parameters employed in present study

Variable	Properties	Unit
Header type	A, B, C, D	-
Flow rate (Q)	0.54, 1.08, 1.62, 2.16	m^3/s
Header length (H)	655.5, 874, 1092.5, 1311	mm

was changed into 655.5, 874, 1092.5, and 1311 mm, and the inlet nozzle position changed into horizontal or vertical side, as shown in Fig. 2. Simulation parameters are summarized in Table 1.

Steady state flow modeling using FLUENT was performed. For flow analysis, continuity (Eq. (1)) and momentum (Eq. (2)) equations were solved with a k-epsilon realizable turbulence model for turbulent analysis used as follows:

$$\nabla \cdot (\rho \vec{v}) = 0 \tag{1}$$

$$\nabla \cdot (\rho \vec{v}\vec{v}) = -\nabla p + \mu(\nabla \vec{v} + \nabla \vec{v}^T) \tag{2}$$

The working fluid was a gaseous mixture of propylene and chlorine in a high temperature reactor (ρ=2.49 kg/m^3, μ=1.7×10^{-5} Pa·s at 540 K). Gas flow rate and gauge pressure were 9,666 kg/h and 236.66 kPa, respectively.

SIMPLEC algorithm was used for pressure-velocity coupling [9], and the solution was iterated until convergence was achieved so that the residual for each equation fell below 10^{-3}.

RESULTS AND DISCUSSION

1. Effects of Header Type

Fig. 3 shows the vector field of velocities in the header of the heat exchanger when the volumetric flow rate of 1.08 m^3/s flows through each header type shown in Fig. 2. For an A-type header,

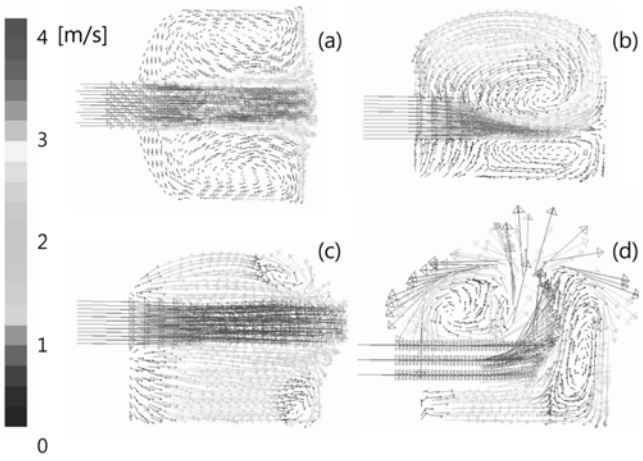

Fig. 3. Velocity vectors of the different header type configurations at the volumetric flow rate of 1.08 m^3/s. (a) A-type header, (b) B-type header, (c) C-type header, and (d) D-type header.

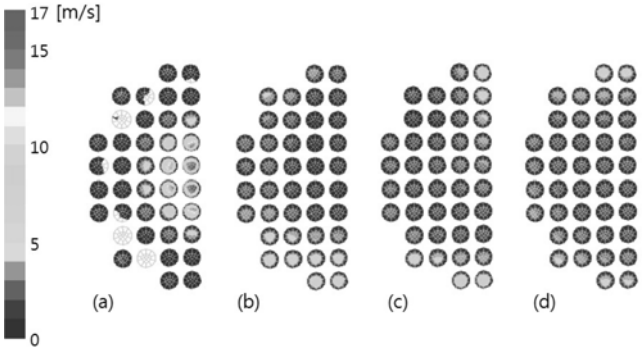

Fig. 4. Variation of velocity in the hole for the four header type configuration. (a) A-type header, (b) B-type header, (c) C-type header, and (d) D-type header.

the velocity vector collided directly against the exit side to pass predominantly through central holes, whereas it collided against the lateral side of the header and then exited in the case of the B- and C-type headers, indicating that B- and C-types are better suited for velocity uniformity. On the other hand, the velocity vector in the case of the D-type header collided against opposite sides of the exit and subsequently passed through the exit, completely owing to the effect of the nozzle shape inserted in the header. In this case, maintenance, repair, and manufacture should be difficult, although it is expected that the velocity uniformity would be much improved.

Fig. 4 shows the velocity distribution in the hole for the four header type configuration. Most of the flow rate in the A-type header, as mentioned above, passed predominantly through central holes leaving several holes through which the flow rate did not flow. In contrast, it was shown that the uniform stream could be observed in the case of the B-type header, as opposed to the A-type header. In addition, the D-type header, where the nozzle was bent at a 90 degree angle, showed more effective gas distribution than the C-type header that, bearing an outside flux entrance, showed better gas distribution than the B-type header.

To estimate the efficiency of each header quantitatively, the pressure drop at the whole part and standard deviation for velocities of

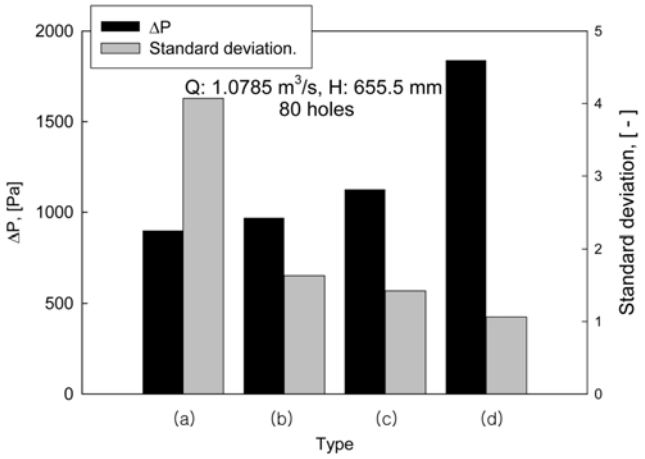

Fig. 5. Variation of standard deviation and pressure drop according to header type under volumetric flow rate of 1.08 m^3/s. (a) A-type header, (b) B-type header, (c) C-type header, and (d) D-type header.

fluid flowing through tubes were calculated and presented in Fig. 5. There was no remarkable difference in pressure drop for A- through C-type headers. However the pressure drop in the D-type header was large compared to the other types because of pressure loss caused by nozzle shape. Since large pressure drop means high power cost when it is operated, B- and C-types, showing uniform distribution as well as low pressure drop, are adequate for application.

2. Effect of Volumetric Flow Rate

Fig. 6 shows the variation of pressure drop and standard deviation of the velocity with the volumetric flow rate. As shown in Fig. 6(a), the pressure drop increased with increasing volumetric flow rate irrespective of header type. The difference in pressure drop among the four header types grew as the volumetric flow rate increased. In Fig. 6(b), it is also shown that the standard deviation increased with increasing volumetric flow rate to make dispersion effectiveness low regardless of header type. The difference between the A-type header and others, as shown in Fig. 6(b), increased with the volumetric flow rate, but the gap between B- and D-type headers decreased. The reason for this can be attributed to the different geo-

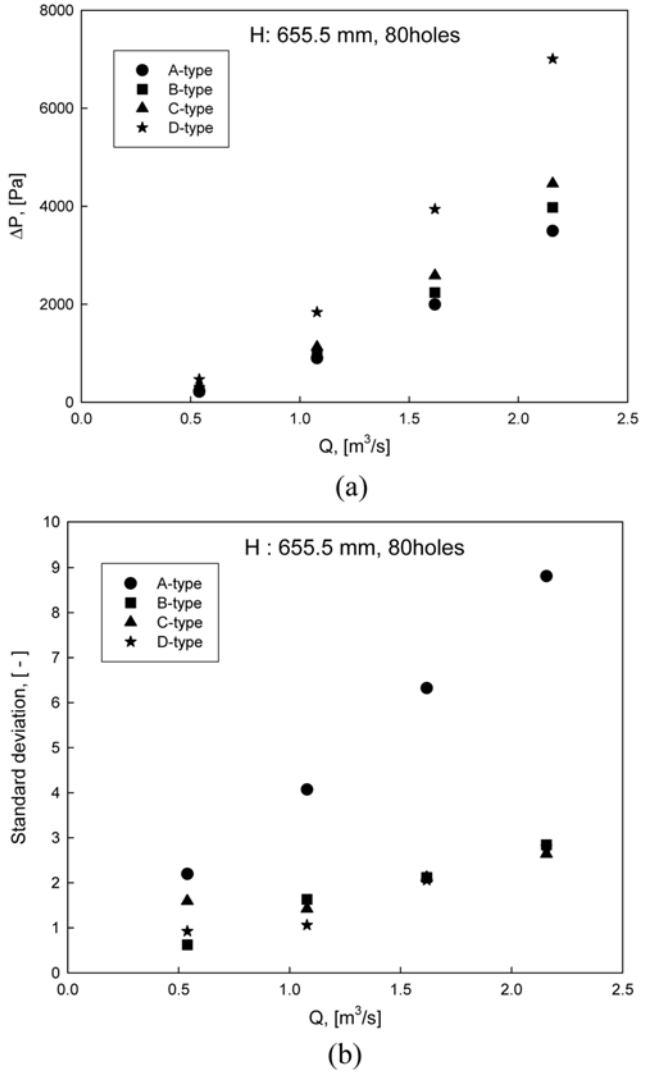

Fig. 6. Comparison of standard deviation and pressure drop for each header type with the volumetric flow rate. (a) pressure drop, and (b) standard deviation.

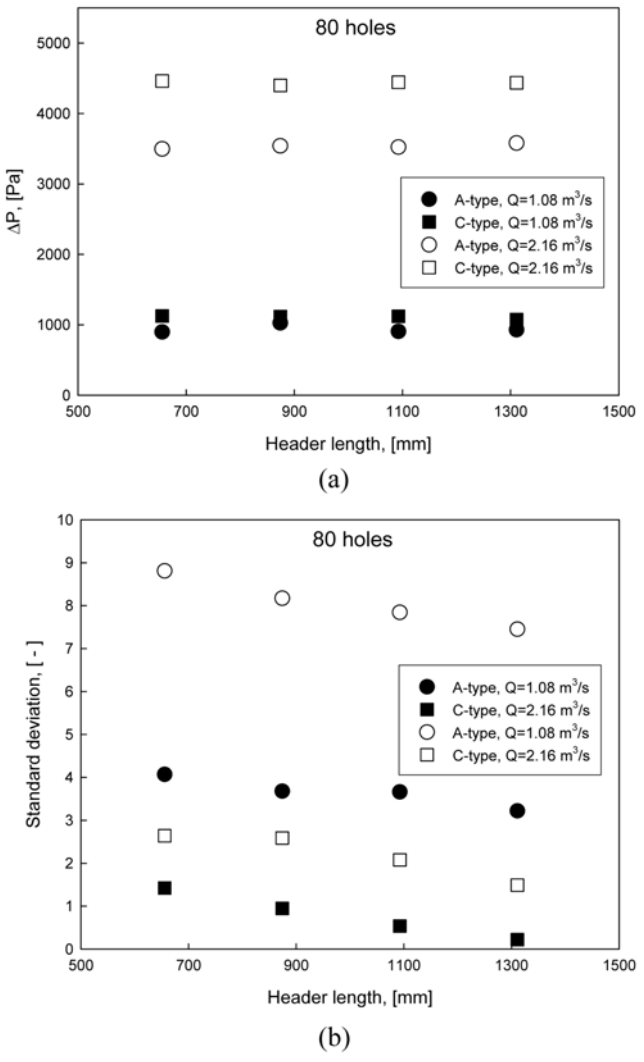

Fig. 7. Comparison of standard deviation and pressure drop for each header type according to the header length. (a) pressure drop, and (b) standard deviation.

metric configurations of each header type that cause the fluid to collide directly against exit side, as with the A-type, and that of other types that make it pass through the exit after collision against the internal walls. Therefore, the A-type is not as effective as the other types because of its higher pressure drop and standard deviation.

3. Effect of Header Length

Fig. 7 shows the effect of header length on pressure drop and standard deviation for each header type. The pressure drop slightly increased with increasing header length, but the standard deviation decreased; thus, it can be expected that the velocity distribution would be uniform with header length. However, a long length of header is not proper due to the occupancy of a large space and a low distribution effectiveness compared to the header type.

4. Case Study

The results of the present study were applied to the header modification of a shell-and-tube heat exchanger, consisting of 754 tubes, at the next step of an allyl chloride reactor. Its header length and volumetric flow rate of mixed gas were 655.5 mm and 1.08 m^3/s, respectively. This heat exchanger has the problem of low efficiency of heat exchange though, owing to the maldistribution among tubes and plugging phenomena of tubes by tar.

If the efficiency of the heat exchanger with 754 tubes was to be calculated using CFD, then long computational times are recommended because of the increase in mesh number caused by the decrease in mesh size. Therefore, the initial investigation focused on how the tube number, ranging from 32 to 112 in the exchanger, affects pressure drop and standard deviation through modeling. Fig. 8(a) shows that the pressure drop increased with increasing number of tubes regardless of header type or volumetric flow rate, and was remarkable at high volumetric flow rates. In the case of the standard deviation shown in Fig. 8(b), it decreased with the tube number irrespective of header type or volumetric flow rate, differing from pressure drop. This effectiveness was predominant in the header with a high standard deviation. However, it was found from Fig. 8 that the tendency of change in pressure drop and standard deviation

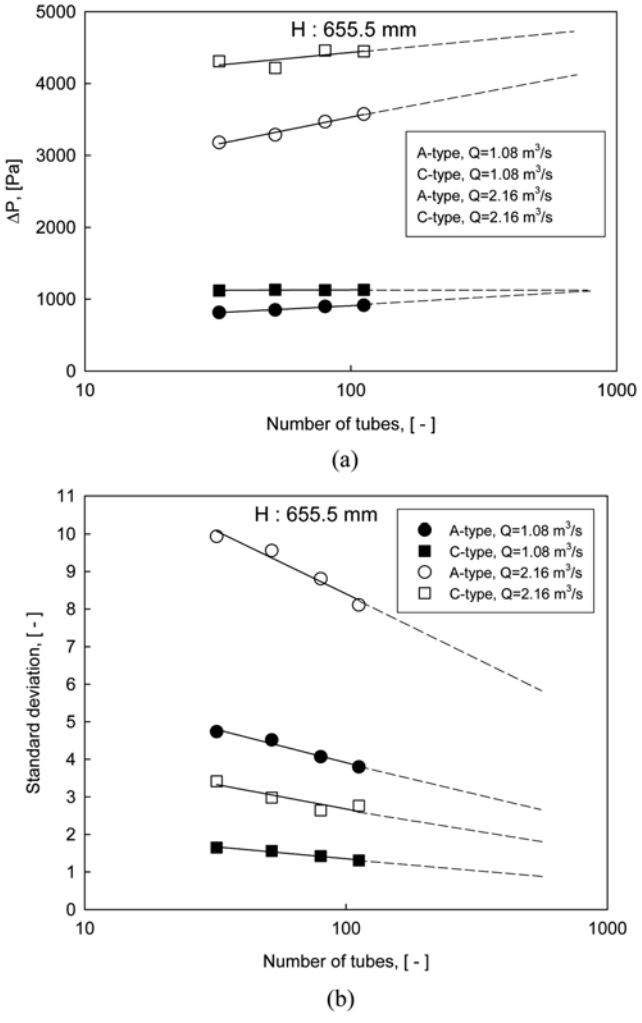

Fig. 8. Effects of number of tubes on the standard deviation and pressure drop of A- and C-header type at each volumetric flow rate. (a) pressure drop, and (b) standard deviation.

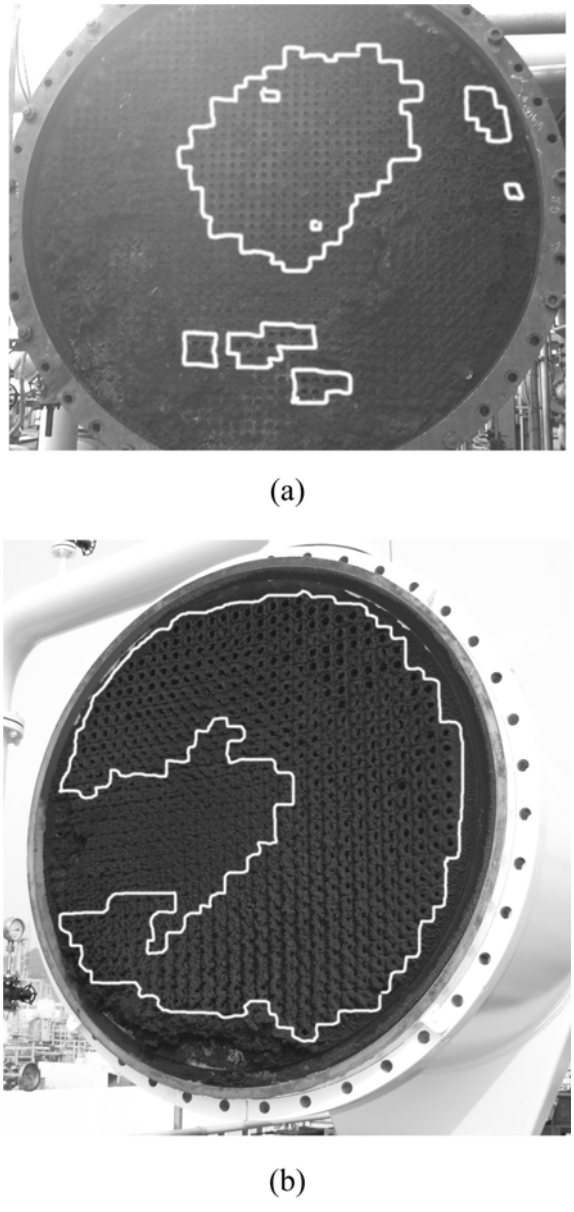

Fig. 9. Effects of header type on plugging phenomena in actual heat exchanger. (a) A-type header, and (b) C-type header.

according to the tube number was the same regardless of header type or volumetric flow rate.

Therefore, in this section, the effect of the C-type header, with a length of 1,311 mm, on the prevention against the plugging phenomenon by tar was compared with that of an A-type header of the same length in an actual exchanger, shown in Fig. 9. Fig. 9(a) shows that most of the outer tubes in the heat exchanger with A-type were plugged. On the other hand, Fig. 9(b) shows that the portion of plugged tubes in the heat exchanger with a C-type header was quite low compared to that in Fig. 9(a). Consequently, a uniform distribution with low power consumption would be achieved when the heat exchanger with C-type header is used.

CONCLUSIONS

CFD modeling was performed to evaluate the flow distribution characteristics in shell-and-tube heat exchangers according to header type. From this present study, the commercially used A-type header was not adequate to distribute the flow uniformly in the heat exchanger, whereas the C-type designed in this study had a good efficiency in flow distribution. Moreover, the optimum position and shape of the inlet nozzle could be proposed for a uniform distribution of a 1.3 m-length header, the very same used for the heat exchange of the commercially viable allyl chloride process.

ACKNOWLEDGMENT

The authors wish to acknowledge support from the Korea Institute of Industrial Technology (2007-A027-00) and the Brain Korean 21 Project in Korea. We appreciate project and equipment support from Gyeonggi province through the GRRC program in Sungkyunkwan University.

NOMENCLATURE

d : tube diameter [m]
H : header length [m]
ΔP : pressure drop [Pa]
ΔP_{av} : average pressure drop [Pa]
Q : volumetric flow rate [m^3/s]
t : pitch length [m]
$\vec{v}$: velocity vector [m/s]
V_o : velocity of tube hole [m/s]
η : velocity ratio [-]
μ : viscosity [Pa·s]
ρ : density of fluid [kg/m^3]

REFERENCES

1. M. S. Peters, K. D. Timmerhaus and R. E. West, *Plant design and economics for chemical engineers*, 5th Ed., McGraw-Hill, Boston (2003).
2. S. Sadik Kakac and H. Liu, *Heat exchangers: selection, rating, and thermal design*, 2nd Edition, CRC Press, Boca Raton, FL (2002).
3. J. K. Lee and S. Y. Lee, *Exp. Therm. and Fluid Sci.*, **28**, 217 (2004).
4. C. Choi, J. H. Lee, H. Kim, N. Cho and J. Lee, *Trans. of the KSME B*, **30**, 780 (2006).
5. A. P. Fraas, *Heat exchanger design*, 2nd Ed., Wiley, New York (1989).
6. S. Lalot, P. Florent, S. K. Lang and A. E. Bergles, *Appl. Therm. Eng.*, **19**, 847 (1999).
7. S. Vist and J. Pettersen, *Exp. Therm. and Fluid Sci.*, **28**, 209 (2004).
8. FLUENT Inc., *FLUENT 6.0 user's guide*, Chap.10 (2001).
9. J. P. Vandoormaal and G. D. Raithby, *Numer. Heat Trans.*, **7**, 147 (1984).